EXACT NONLINEAR FOURTH-ORDER EQUATION FOR TWO COUPLED OSCILLATORS: METAMORPHOSES OF RESONANCE CURVES

Jan Kyzioł

Department of Mechatronics and Mechanical Engineering
Kielce University of Technology
Al. 1000-lecia PP 7, 25-314 Kielce, Poland

Andrzej Okniński

Department of Management and Computer Modelling, Physics Division
Kielce University of Technology
Al. 1000-lecia PP 7, 25-314 Kielce, Poland

(Received November 12, 2012; revised version received December 4, 2012)

We study dynamics of two coupled periodically driven oscillators. The internal motion is separated off exactly to yield a nonlinear fourth-order equation describing inner dynamics. Periodic steady-state solutions of the fourth-order equation are determined within the Krylov–Bogoliubov–Mitropolsky approach and we compute the corresponding amplitude profiles. In the present paper, we explore rich variety of singular points of the amplitude profiles. Metamorphoses of these curves induced by changes of control parameters and the corresponding changes of dynamics are studied.

DOI:10.5506/APhysPolB.44.35
PACS numbers: 05.45.Xt, 02.40.Xx

1. Introduction

In this work, we study dynamics of two coupled oscillators, one of which is driven by an external periodic force. Equations governing dynamics of such system are of the form

$$\left.\begin{array}{l} m_1\ddot{x}_1 - V_1\left(\dot{x}_1\right) - R_1\left(x_1\right) + V_2\left(\dot{x}_2 - \dot{x}_1\right) + R_2\left(x_2 - x_1\right) = F\left(t\right) \\ m_2\ddot{x}_2 - V_2\left(\dot{x}_2 - \dot{x}_1\right) - R_2\left(x_2 - x_1\right) = 0 \end{array}\right\}, \quad (1.1)$$

where R_1, V_1 and R_2, V_2 are nonlinear elastic restoring force and nonlinear force of internal friction for mass m_1 and mass m_2, respectively. Dynamic

vibration absorber, consisting of a (generally small) mass m_2, attached to the primary vibrating system of (typically larger) mass m_1 is a generic mechanical model described by (1.1) [1, 2].

Dynamics of coupled periodically driven oscillators is very complicated [3–8]. Starting from equations (1.1) and the following simplifying assumptions

$$F(t) = f\cos(\omega t)\,, \qquad R_1(x_1) = -\alpha_1 x_1\,, \qquad V_1(\dot{x}_1) = -\nu_1\dot{x}_1 \tag{1.2}$$

we derive the exact 4th-order nonlinear equation for internal motion. Applying the Krylov–Bogoliubov–Mitropolsky (KBM) method to this equation, we compute and study the corresponding nonlinear resonances. More exactly, we investigate the amplitude profiles (resonance curves) $A(\omega)$, *i.e.* dependence of the amplitude on the frequency ω, given implicitly by the KBM method as $L(A, \omega; a, b, \ldots) = 0$, where $a, b, \ldots$ are some parameters and L a polynomial function.

Metamorphoses of the resonance curves $A(\omega)$ induced by changes of the control parameters, leading to new nonlinear phenomena, have been studied in the case of the approximate effective equation (this approximation performs well for $\frac{m_2}{m_1} \ll 1$ [9, 10]) within the theory of algebraic curves since they occur in the neighbourhoods of singular points of $A(\omega)$ [11–13].

In the present paper, we apply our approach, based on the theory of algebraic curves and described in our recent papers [11–13], to a new model. More exactly, we study the exact 4th-order equation for internal motion which has been derived from Eqs. (1.1), *cf.* [9, 10]. The resonance curves are more complicated than in the case of effective equation and hence more complicated metamorphoses are possible. The aim of the present paper is to explore these possibilities. For example, we address the problem of algebraic curves with two singular points. This is a more difficult global problem since a single singular point needs local methods only.

The paper is organized as follows. In the next section, the exact 4th-order equation for the internal motion in non-dimensional form is presented. In Sec. 3, equation for resonance curves $A(\omega)$ is derived via the Krylov–Bogoliubov–Mitropolsky approach. Since the KBM method was originally designed to study second-order equations, we had to prepare the 4th-order equation properly to remove secular terms. In Sec. 4, theory of algebraic curves is used to compute singular points on these amplitude profiles. In Sec. 5, new results are presented. We compute for the first time a resonance curve with two singular points, a curve with a degenerate singular point as well as the corresponding bifurcation diagrams. Our results are summarized in the last section.

2. Exact equation for internal motion

In new variables, $x \equiv x_1$, $y \equiv x_2 - x_1$, equations (1.1), (1.2) can be written as

$$\left.\begin{array}{l} m\ddot{x} + \nu\dot{x} + \alpha x + V_e(\dot{y}) + R_e(y) = f\cos(\omega t) \\ m_e(\ddot{x} + \ddot{y}) - V_e(\dot{y}) - R_e(y) = 0 \end{array}\right\}, \tag{2.1}$$

where $m \equiv m_1$, $m_e \equiv m_2$, $\nu \equiv \nu_1$, $\alpha \equiv \alpha_1$, $V_e \equiv V_2$, $R_e \equiv R_2$.

We can eliminate variable x in (2.1) to obtain the following exact equation for relative motion

$$\widehat{L}\left(\mu\ddot{y} - V_e(\dot{y}) - R_e(y)\right) + \epsilon m_e \widehat{K} y = F\cos(\omega t)\,, \tag{2.2}$$

where $\widehat{L} = M\frac{d^2}{dt^2} + \nu\frac{d}{dt} + \alpha$, $\widehat{K} = \left(\nu\frac{d}{dt} + \alpha\right)\frac{d^2}{dt^2}$, $F = m_e\omega^2 f$, $\epsilon = m_e/M$, $\mu = mm_e/M$ and $M = m + m_e$ [9, 10], see also Ref. [14], where separation of variables for a more general system of coupled equations was described. For small ϵ, we can reject the term proportional to ϵ to obtain the approximate (effective) equation which can be integrated partly to yield the effective equation [9, 10]. This effective model was also investigated in [8], where limiting phase trajectories approach was used.

In what follows, we shall assume that $R_e(y)$, $V_e(\dot{y})$ are nonlinear

$$R_e(y) = -\alpha_e y - \gamma_e y^3\,, \qquad V_e(\dot{y}) = -\nu_e\dot{y} + \lambda_e\dot{y}^3\,. \tag{2.3}$$

In this work, we shall investigate the exact equation (2.2). Introducing nondimensional time τ and rescaling variable y

$$\tau = t\bar{\omega}\,, \qquad z = y\sqrt{\frac{\gamma_e}{\alpha_e}}\,, \tag{2.4}$$

where

$$\bar{\omega} = \sqrt{\frac{\alpha_e}{\mu}}\,, \tag{2.5}$$

we get

$$\widehat{\mathcal{L}}\left(\frac{d^2z}{d\tau^2} + h\frac{dz}{d\tau} - b\left(\frac{dz}{d\tau}\right)^3 + z + z^3\right) + \kappa\widehat{\mathcal{K}}z = \frac{\kappa}{\kappa+1}G\Omega^2\cos(\Omega\tau)\,, \tag{2.6}$$

where $\hat{\mathcal{L}}$, $\widehat{\mathcal{K}}$ are linear operators

$$\hat{\mathcal{L}} = \frac{d^2}{d\tau^2} + H\frac{d}{d\tau} + a\,, \quad \widehat{\mathcal{K}} = \left(H\frac{d}{d\tau} + a\right)\frac{d^2}{d\tau^2}\,, \tag{2.7}$$

and nondimensional constants are given by

$$h = \frac{\nu_e}{\mu\bar{\omega}}, \qquad b = \frac{\lambda_e}{\gamma_e}\bar{\omega}^3, \qquad H = \frac{\nu}{M\bar{\omega}}, \qquad \Omega = \frac{\omega}{\bar{\omega}},$$
$$G = \frac{1}{\alpha_e}\sqrt{\frac{\gamma_e}{\alpha_e}}f, \qquad \kappa = \frac{m_e}{m}, \qquad a = \frac{\alpha\mu}{\alpha_e M}. \tag{2.8}$$

3. Nonlinear resonances via Krylov–Bogoliubov–Mitropolsky method

We apply the Krylov–Bogoliubov–Mitropolsky (KBM) perturbation approach [15, 16] to the exact nonlinear fourth-order equation (2.6) describing internal motion of the small mass. The equation (2.6) is written in the following form

$$\widehat{\mathcal{L}}\left(\frac{d^2z}{d\tau^2} + \Omega^2 z\right) + \varepsilon\left(\sigma\widehat{\mathcal{L}}z + g\left(z,\dot{z}\right)\right) = 0, \tag{3.1}$$

where $\hat{\mathcal{L}}$, $\widehat{\mathcal{K}}$ are defined in (2.7) and $\varepsilon g\left(z,\dot{z}\right)$ is given by

$$\varepsilon g = \widehat{\mathcal{L}}\left(h\frac{dz}{d\tau} - b\left(\frac{dz}{d\tau}\right)^3 + z + z^3\right) - \Theta^2\widehat{\mathcal{L}}z + \kappa\widehat{\mathcal{K}}z - \lambda\Omega^2\cos\left(\Omega\tau\right), \tag{3.2}$$

where $\lambda = \frac{\kappa}{\kappa+1}G$ and

$$\Theta^2 - \Omega^2 = \varepsilon\sigma. \tag{3.3}$$

Equation (3.1) was prepared in such a way that for $\varepsilon = 0$ the general solution is $z\left(\tau\right) = A\cos\left(\Omega\tau + \varphi\right) + C_1\exp\left(-\frac{1}{2}H_-\tau\right) + C_2\exp\left(-\frac{1}{2}H_+\tau\right)$, where $H_- \equiv H - \sqrt{\Delta}$, $H_+ \equiv H + \sqrt{\Delta}$, $\Delta = H^2 - 4a$, with constant and arbitrary A, φ, C_1, C_2. We note that this solution for $H, a > 0$ does not contain secular terms and $z\left(\tau\right) \longrightarrow A\cos\left(\Omega\tau + \varphi\right)$ for $\tau \longrightarrow \infty$.

We shall now look for $1:1$ resonance using the KBM method. For small nonzero ε, the solution of Eqs. (3.1)–(3.3) and (2.3) is sought in form

$$z = A\cos\left(\Omega\tau + \varphi\right) + \varepsilon z_1\left(A,\varphi,\tau\right) + \ldots \tag{3.4}$$

with slowly varying amplitude and phase

$$\frac{dA}{d\tau} = \varepsilon M_1\left(A,\varphi\right) + \ldots, \tag{3.5}$$
$$\frac{d\varphi}{d\tau} = \varepsilon N_1\left(A,\varphi\right) + \ldots. \tag{3.6}$$

Computing now derivatives of z from Eqs. (3.4), (3.5), (3.6) and substituting to Eqs. (3.1)–(3.3), (2.3) and eliminating secular terms and demanding $M_1 = 0$, $N_1 = 0$, we obtain the following equations for the amplitude and phase of steady states

$$-\Omega A\left(p\Omega^2 - q\right) + \tfrac{3}{4}\Omega A^3\left(H - ba\Omega^2 + b\Omega^4\right) + \lambda\Omega^2 \sin\varphi = 0\,, \quad (3.7)$$

$$-A\left(\Omega^4 - r\Omega^2 + a\right) - \tfrac{3}{4}A^3\left(a - \Omega^2 + Hb\Omega^4\right) + \lambda\Omega^2\cos\varphi = 0\,, \quad (3.8)$$

where $\lambda = \frac{\kappa}{\kappa+1}G$, $p = h + H(\kappa+1)$, $q = ah + H$, $r = hH + a(\kappa+1) + 1$.

Solving the system of equations (3.7), (3.8), we get the implicit expressions for the amplitude $A(\Omega)$ and the phase $\varphi(\Omega)$

$$A(\Omega) = \lambda\frac{\Omega^2}{\sqrt{C^2 + D^2}}\,, \quad (3.9a)$$

$$\tan\varphi = \frac{C}{D}\,, \quad (3.9b)$$

$$C = \Omega A(\Omega)\left(p\Omega^2 - q\right) - \tfrac{3}{4}\Omega A^3(\Omega)\left(H - ba\Omega^2 + b\Omega^4\right)\,, \quad (3.9c)$$

$$D = A(\Omega)\left(\Omega^4 - r\Omega^2 + a\right) + \tfrac{3}{4}A^3(\Omega)\left(a - \Omega^2 + Hb\Omega^4\right)\,. \quad (3.9d)$$

Equation for the correcting term z_1 is of form

$$\widehat{\mathcal{L}}\left(\frac{d^2 z_1}{d\tau^2} + \Omega^2 z_1\right) = \tfrac{3}{4}H\Omega A^3\sin\Phi + \tfrac{1}{4}A^3\left((3+a)\Omega^2 - 3b\right)\cos\Phi\,, \quad (3.10)$$

where $\Phi \equiv 3\Omega\tau + 3\varphi(\Omega)$. Solving Eq. (3.10) and substituting to (3.4), we get finally

$$z = A(\Omega)\cos(\Omega\tau + \varphi) - \frac{1}{32}A^3(\Omega)\, b\Omega\sin(\Phi) + \frac{1}{32\Omega^2}A^3(\Omega)\cos(\Phi)\,, \quad (3.11)$$

where $A(\Omega)$, $\varphi(\Omega)$ are given by Eqs. (3.9).

4. General properties of the function $A(\Omega)$

After introducing new variables, $\Omega^2 = X$, $A^2 = Y$, the equations (3.9a), (3.9c), (3.9d) defining the amplitude profile read

$$L(X, Y; a, b, h, H, \kappa, J) \stackrel{df}{=} XY\left(pX - q - \tfrac{3}{4}Y\left(H - abX + bX^2\right)\right)^2$$
$$+Y\left(X^2 - rX + a + \tfrac{3}{4}Y\left(a - X + bHX^2\right)\right)^2 - JX^2 = 0\,, \quad (4.1)$$

where, as before, $p = h + H(\kappa+1)$, $q = ah + H$, $r = hH + a(\kappa+1) + 1$.

A new parameter J is a renormalized G^2, $J = \lambda^2 = \left(\frac{\kappa}{\kappa+1}\right)^2 G^2$. To obtain the corresponding expression for the effective equation, one can put $G = \gamma\frac{\kappa+1}{\kappa}$ so that $J = \gamma^2$ and then substitute $\kappa = 0$.

Singular points of $L(X, Y)$ are computed from equations [17]

$$L = 0\,, \tag{4.2a}$$

$$\frac{\partial L}{\partial X} = 0\,, \tag{4.2b}$$

$$\frac{\partial L}{\partial Y} = 0\,. \tag{4.2c}$$

We can eliminate J from Eqs. (4.2a), (4.2b) computing $L - \frac{1}{2}X\frac{\partial L}{\partial X} = \frac{1}{32}YK$, where

$$\begin{aligned} K = {} & -18b^2H^2X^4Y^2 - 24a^2(\kappa+1)XY + 24bhH^2X^3Y + 32X^3 \\ & -18aXY^2 - 48aXY + 32HhX^3 + 32a^2 - 27b^2X^5Y^2 + 16H^2X \\ & -32aX - 32a^2(\kappa+1)X + 32a(\kappa+1)X^3 + 9H^2XY^2 + 24X^3Y \\ & +24H^2XY + 48a^2Y + 18a^2Y^2 + 48hbX^4Y - 9a^2b^2X^3Y^2 - 32X^4 \\ & -16h^2X^3 + 16a^2h^2X - 16(\kappa+1)^2H^2X^3 + 48bH(\kappa+1)X^4Y \\ & -32hH(\kappa+1)X^3 - 48abhX^3Y - 48bHX^4Y + 36ab^2X^4Y^2 \end{aligned} \tag{4.3}$$

to obtain simplified equations

$$K = 0\,, \tag{4.4}$$

$$\frac{\partial L}{\partial Y} = 0 \tag{4.5}$$

from which X, Y can be computed as functions of parameters a, b, h, H, κ and, finally, J can be computed from the last equation

$$\frac{\partial L}{\partial X} = 0\,. \tag{4.6}$$

Equations (4.4), (4.5), (4.6) are still very complicated making analytical investigation virtually impossible. We shall thus solve these equations numerically.

5. Computational results

In the present section, singular points of amplitude profiles — solutions of Eqs. (4.4), (4.5), (4.6) — are studied. More exactly, resonance curves with one singular point, two singular points on one curve, and with degenerate singular point are presented and metamorphoses of bifurcation diagrams are shown.

5.1. Amplitude profiles with one singular point

We have computed singular points for the following values of control parameters: $\kappa = 0.05$, $b = -0.001$, $H = 0.4$, $a = 5$, $h = 0.5$ obtaining four physical solutions (*i.e.* with $X > 0$, $Y > 0$, $J > 0$).

TABLE I

X	Y	J	n
2.170 051 157	1.357 255 661	1.656 917 694	1
4.835 083 103	4.192 055 014	1.036 434 992	2
2.798 801 078	1.237 140 868	1.814 387 388	3
4.153 001 386	4.680 111 331	0.963 352 654	4

The first two solutions correspond to self-intersections, see Fig. 1, while the second pair represents isolated points.

Metamorphoses of bifurcation diagrams which occur in the neighbourhood of self-intersections for the exact fourth-order equation are, for small κ, qualitatively similar to those studied for the case of 1 : 1 resonance in the effective equation in [11, 13] and are not shown here.

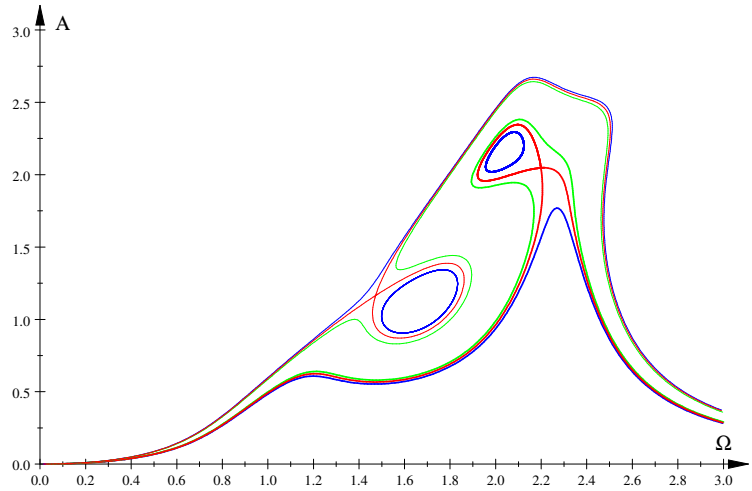

Fig. 1. Amplitude profiles with singular points, $\kappa = 0.05$, $b = -0.001$, $H = 0.4$, $a = 5$, $h = 0.5$, $J = 1.656\,918$ (left self-intersection, thin black/red curve, $n = 1$ in Table I) and neighbouring curve (thin light grey/blue and grey/green lines); $J = 1.036\,435$ (right self-intersection, medium black/red curve, $n = 2$ in Table I) and neighbouring curves (medium light grey/blue and grey/green lines).

5.2. Amplitude profiles with two singular points

It is possible, tuning the parameters properly, to obtain amplitude profile with two singular points.

Let, as before, $\kappa = 0.05$, $b = -0.001$, $a = 5$, $h = 0.5$, H being arbitrary. We can compute, for some H, from (4.4), (4.5) $X(H)$, $Y(H)$, then from Eq. (4.6) we get $J_1(H)$ and $J_2(H)$ corresponding to two curves with one intersection each. The condition for a curve with two intersections is $J_1 = J_2$ for some H.

To find this value of H, we compute J_1, J_2 for two values of H, $H_0 = 0.40$, $H_1 = 0.55$, and use linear extrapolation to compute $H = H_{\rm cr}$ such that $J_1(H_{\rm cr}) = J_2(H_{\rm cr})$. In one step of this procedure, we compute new value of $H^{(i+2)}$ from known $H^{(i)}$, $J_1^{(i)}$, $J_2^{(i)}$ and $H^{(i+1)}$, $J_1^{(i+1)}$, $J_2^{(i+1)}$ solving linear system of equations for $\alpha^{(i,i+1)}$, $\beta^{(i,i+1)}$

$$\begin{aligned} J_1^{(i)} - J_2^{(i)} &= H^{(i)}\alpha^{(i,i+1)} + \beta^{(i,i+1)}, \\ J_1^{(i+1)} - J_2^{(i+1)} &= H^{(i+1)}\alpha^{(i,i+1)} + \beta^{(i,i+1)}, \end{aligned} \tag{5.1}$$

where $i = 0, 1, 2, \ldots$. Then, the next value of $H^{(i+2)}$ is computed as $H^{(i+2)} = -\frac{\beta^{(i,i+1)}}{\alpha^{(i,i+1)}}$. The convergence is quite fast, see Fig. 2 and Tables II, III, where convergence of two curves with one singular point to one curve with two singular points is shown.

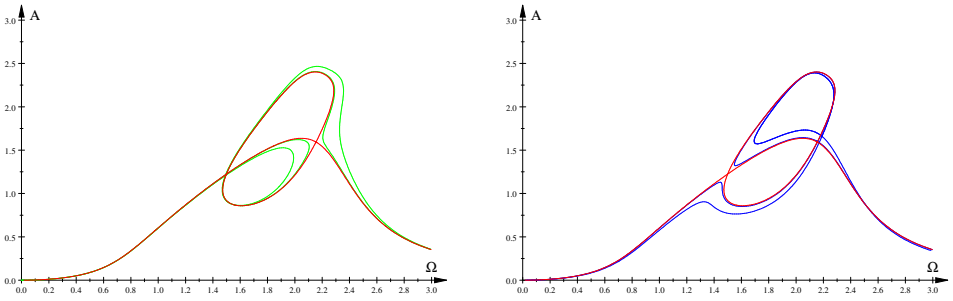

Fig. 2. Convergence of amplitude profiles to critical amplitude profile with two singular points (thick/red curves): convergence of curves from Table II (left figure, thin/green curves), and from Table III (right figure, thin/blue).

Bifurcation diagrams computed for parameters in the neighbourhood of such resonance curve display presence of two singular points, see Fig. 3. The parameters are $\kappa = 0.05$, $b = -0.001$, $a = 5$, $h = 0.5$ in both cases, and $J_* = 1.745\,481\,261$, $H_* = 0.6054$ for Fig. 3 (left), and $J = 1.740\,481\,261$, $H = 0.6034$ for Fig. 3 (right).

TABLE II

$X_1^{(i)}$	$Y_1^{(i)}$	$J_1^{(i)}$	$H^{(i)}$	i
2.170 051 157	1.357 255 661	1.656 917 694	0.40	0
2.222 181 140	1.452 883 358	1.736 397 285	0.55	1
2.250 807 092	1.503 767 806	1.775 975 009	0.611 498 955	2
2.247 348 900	1.497 675 627	1.771 343 329	0.604 644 433	3
2.247 330 153	1.497 642 563	1.771 318 111	0.604 606 880	4
2.247 330 182	1.497 642 613	1.771 318 150	0.604 606 937	5

TABLE III

$X_2^{(i)}$	$Y_2^{(i)}$	$J_2^{(i)}$	$H^{(i)}$	i
4.835 083 103	4.192 055 014	1.036 434 992	0.40	0
4.793 018 228	2.753 798 647	1.555 975 411	0.55	1
4.620 272 267	2.513 582 261	1.798 606 879	0.611 498 955	2
4.641 565 672	2.538 879 342	1.771 466 643	0.604 644 433	3
4.641 680 711	2.539 018 448	1.771 317 923	0.604 606 880	4
4.641 680 536	2.539 018 236	1.771 318 150	0.604 606 937	5

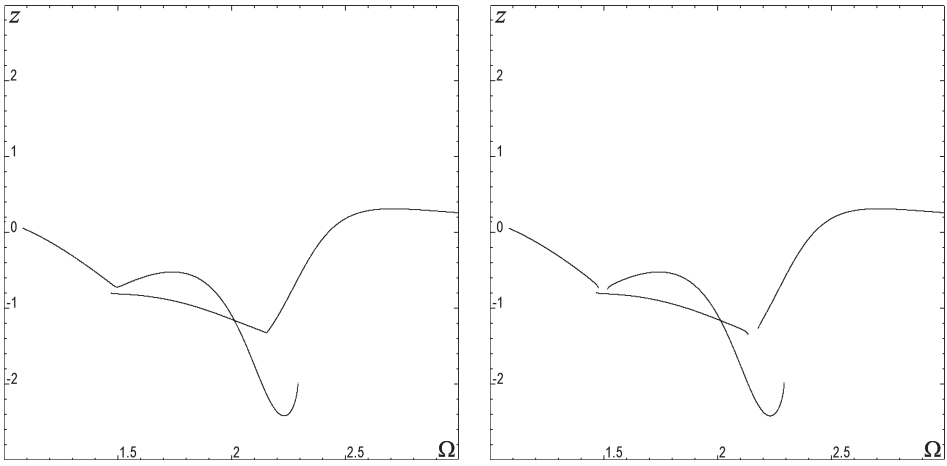

Fig. 3. Bifurcation diagrams. Left: The amplitude profile as singular point with two cusps. Right: The nonsingular curve with two gaps.

Let us notice that singular points of $A(\Omega)$ which show up in the bifurcation diagram as two cusps, *cf.* Fig. 3 (left) , appear at slightly different values of J, H than in Tables II, III above, $i = 5$. These differences ($J_* = 1.745\,481\,261$, $H_* = 0.6054$ instead of $J_{\rm cr} = 1.771\,318\,150$, $H_{\rm cr} = 0.604\,606\,937$) provide the test of accuracy of the KBM method. The diagrams correspond to amplitude profiles shown in Fig. 4. Singular points in Fig. 4 (left) are those listed in Tables II, III, $i = 5$ (note that $X = \Omega^2$, $Y = A^2$).

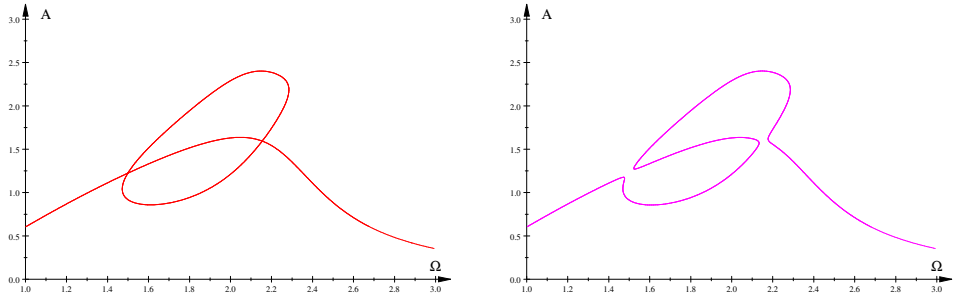

Fig. 4. The amplitude profile with two singular points (left figure, black/red) and nonsingular curve (right figure, grey/magenta). Parameters are $\kappa = 0.05$, $b = -0.001$, $H = 0.4$, $a = 5$, $h = 0.5$ and $J = J_{\rm cr}$, $H = H_{\rm cr}$ for the left figure, $J = 1.766\,318\,150$, $H = 0.602\,606\,937$ for the right figure.

More exactly, singular points (A, Ω), *i.e.* self-intersections visible in Fig. 4 (left), are $(1.499\,111,\ 1.223\,782)$ and $(2.154\,456,\ 1.593\,430)$.

5.3. Merging two singular points into a single degenerate point

It is possible, by smooth change of the parameters, to merge two singular points lying on the red curve in Fig. 2. The resulting singular point is degenerate, *i.e.* fulfils the following set of equations [17]

$$\begin{aligned} L &= 0\,, & \frac{\partial L}{\partial X} &= 0\,, & \frac{\partial L}{\partial Y} &= 0\,, \\ \frac{\partial^2 L}{\partial X^2} &= 0\,, & \frac{\partial^2 L}{\partial X \partial Y} &= 0\,, & \frac{\partial^2 L}{\partial Y^2} &= 0\,, \end{aligned} \tag{5.2}$$

where $L(X, Y)$ is given by (4.1).

Solving Eqs. (5.2) for $\kappa = 0.05$, $J = 1.771\,318\,150$ (these two parameters correspond to the parameters of the critical red curve with two singular points), we get $X = 3.113\,090\,974$, $Y = 2.087\,620\,813$, $h = 0.548\,982\,679$, $a = 4.538\,990\,962$, $b = -1.718\,542\,532 \times 10^{-2}$, $H = 0.644\,095\,068$, see Fig. 5.

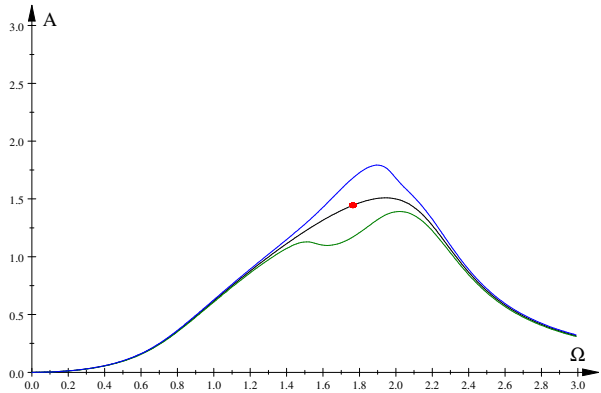

Fig. 5. Amplitude profile with degererate singular point (black/red dot) and two neighbouring curves (dark grey/green and grey/blue).

Bifurcation diagrams computed in the neighbourhood of the degenerate singular point depend sensitively on small changes of parameters, Fig. 6.

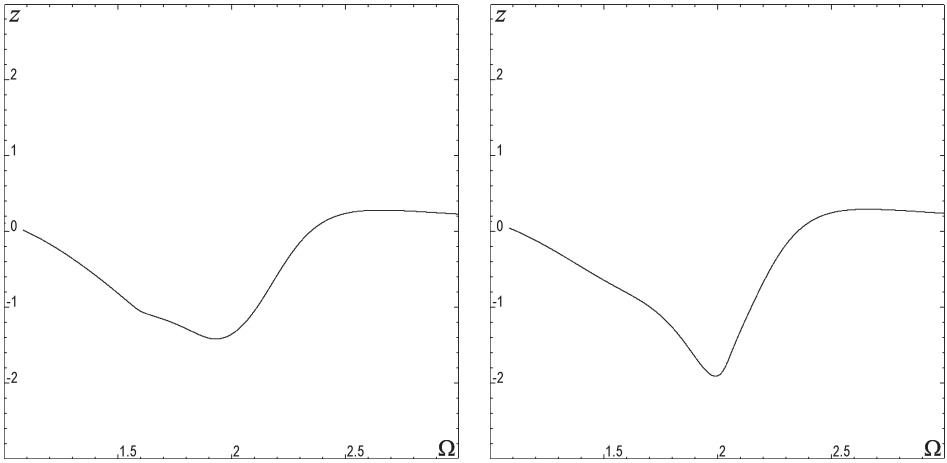

Fig. 6. Metamorphosis of the bifurcation diagrams near amplitude profile with degenerate singular point.

6. Summary and discussion

In this work, we have studied dynamics of two coupled periodically driven oscillators. The inner motion of this system has been described by the exact fourth-order equation (2.2) (or (2.6) in nondimensional form). Applying the KBM method, we have computed approximate resonance curves (amplitude

profiles) $A(\Omega)$. Although the KBM method is basically used for the second-order equations, we managed to apply it to the fourth-order equation since it was possible to eliminate secular terms and impose steady-state conditions. Dependence of the amplitude A on the forcing frequency Ω is complex since $A(\Omega)$ is defined implicitly as an algebraic curve, $L(X,Y)=0$, see Eq. (4.1), with polynomial function L depending on variables $X=\Omega^2$, $Y=A^2$ and control parameters a, b, h, H, κ, J in a complicated manner.

In our previous paper, we stressed that near singular points of algebraic curves, defining amplitude profiles, metamorphoses of bifurcation diagrams (and hence of dynamics) take place. In the present paper, we have studied three cases of singular points of the resonance curves defined by Eq. (4.1): *(i)* the case of one singular point (Sec. 5.1), *(ii)* the case of two singular points on one resonance curve (Sec. (5.2)), *(iii)* the case of degenerate singular point (Sec. (5.3)). Indeed, dynamics of the system (2.6) changes significantly in the neighbourhood of singular points of resonance curve $L(X,Y)=0$. Singular points described in Sec. 5 are just the tip of the iceberg and thus, we are going to study multitude of singular points of amplitude profiles (4.1) in our future work.

REFERENCES

[1] J.P. Den Hartog, *Mechanical Vibrations*, 4th edition, Dover Publications, New York 1985.

[2] S.S. Oueini, A.H. Nayfeh, J.R. Pratt, *Arch. Appl. Mech.* **69**, 585 (1999).

[3] W. Szemplińska-Stupnicka, *The Behavior of Non-linear Vibrating Systems*, Kluver Academic Publishers, Dordrecht 1990.

[4] J. Awrejcewicz, *Bifurcation and Chaos in Coupled Oscillators*, World Scientific, New Jersey 1991.

[5] J. Kozłowski, U. Parlitz, W. Lauterborn, *Phys. Rev.* **E51**, 1861 (1995).

[6] K. Janicki, W. Szemplińska-Stupnicka, *J. Sound. Vibr.* **180**, 253 (1995).

[7] A.P. Kuznetsov, N.V. Stankevich, L.V. Turukina, *Physica D* **238**, 1203 (2009).

[8] J. Awrejcewicz, R. Starosta, *Theor. Appl. Mech. Lett.* **2**, 043002 (2012).

[9] A. Okniński, J. Kyzioł, *Mach. Dyn. Prob.* **29**, 107 (2005).

[10] A. Okniński, J. Kyzioł, *Differ. Equ. Nonlinear Mech.* **2006**, 56146 (2006).

[11] J. Kyzioł, A. Okniński, *Acta Phys. Pol. B* **42**, 2063 (2011).

[12] J. Kyzioł, A. Okniński, *Acta Phys. Pol. B* **43**, 1275 (2012).

[13] J. Kyzioł, A. Okniński, *Differ. Equ. Dyn. Syst.* **21**, 159 (2013).

[14] R. Starosta, J. Awrejcewicz, L. Manevitch, in: *Dynamical Systems. Analytical/Numerical Methods, Stability, Bifurcation and Chaos*, J. Awrejcewicz, M. Kaźmierczak, P. Olejnik, J. Mrozowski, Editors, The University of Łódź Publishing House, Łódź 2011, pp. 79–84.

[15] A.H. Nayfeh, *Introduction to Perturbation Techniques*, John Wiley & Sons, New York 1981.

[16] J. Awrejcewicz, V.A. Krysko, *Introduction to Asymptotic Methods*, Chapman and Hall (CRC Press), New York 2006.

[17] C.T.C. Wall, *Singular Points of Plane Curves*, Cambridge University Press, New York 2004.